Petrographic and geochemical characteristics of upper Aptian calc-alkaline volcanism in San Miguel de Allende, Guanajuato state, Mexico

Luis Enrique Ortiz-Hernández [1,2*], Kinardo Flores-Castro [1], and Otilio Arturo Acevedo-Sandoval [1]

[1]Centro de Investigaciones en Ciencias de la Tierra, Universidad Autónoma del Estado de Hidalgo, Carretera Pachuca-Tulancingo Km. 4.5, 42184, Pachuca, Hgo., México.
[2] Instituto Politécnico Nacional, Sección de Estudios de Posgrado e Investigación, ESIA-Unidad Ticomán, Avenida Ticomán 600, Col. San José Ticomán. Del. Gustavo A. Madero, 07340 México, D.F.
** leoh@uaeh.reduaeh.mx*

ABSTRACT

A volcanic sequence formed by calc-alkaline basalts and basaltic andesites interbedded with pelagic limestones, black shales, radiolarites, and epiclastic rocks that are in tectonic contact with flysch-like strata, is reported in the vicinity of San Miguel de Allende, in Guanajuato state. An upper Aptian age is suggested by paleontological evidence. The sequence is interpreted as the eastern remnant of an allochthonous, lower Cretaceous volcanic stage in central Mexico.

Keywords: Guerrero terrane, calc-alkaline volcanism, petrography, geochemistry, Guanajuato, Mexico.

RESUMEN

Se consigna la ocurrencia de una secuencia volcánica formada de basaltos y andesitas basálticas calcialcalinos intercalados con calizas pelágicas, pizarras negras, radiolaritas y rocas epiclásticas que están en contacto tectónico con rocas flyschoides, en las inmediaciones de San Miguel de Allende, en el estado de Guanajuato. Su edad del Aptiano Superior es sugerida en base a la evidencia paleontológica. Esta secuencia se considera como el testigo más oriental de un evento de vulcanismo del Cretácico Inferior en posición alóctona, presente en México central.

Palabras clave: Terreno Guerrero, vulcanismo calcialcalino, petrografía, geoquímica, Guanajuato, México.

INTRODUCTION

The Guerrero suspect terrane of south-central Mexico is characterized by the presence of Upper Jurassic-Early Cretaceous volcano-plutonic and volcanosedimentary sequences formed in an intra-oceanic arc environment (Monod *et al*., 1990; Ortiz-Hernández *et al*., 1991a, Lapierre *et al*., 1992; Talavera-Mendoza *et al*., 1995). The arc rocks either rest unconformably on partially metamorphosed Triassic-Jurassic assemblages, formed by turbidites, basalts, graywackes, and blocks of chert and limestone (Centeno-García, 1994), or are to be found in tectonic contact with Lower Cretaceous basin rocks from the Arperos Formation (Monod *et al*., 1990; Freydier *et al*., 2000).

In central Mexico, the allochthonous outcrops of the Guerrero terrane have been exposed by Neogene grabens crosscutting the Mesozoic basement, as is the case of the volcano-plutonic and volcanosedimentary sequences of the Sierra de Guanajuato, located between the Guanajuato mining district and the town of Comanja de Corona, in Jalisco state. Other isolated outcrops of this

terrane are found in Zacatecas state, in the Fresnillo mining district (de Cserna, 1976) or in the Saucito and Zacatecas areas where pillow lavas are interbedded with pelagic limestone, chert and volcaniclastic rocks.

The occurrence and the petrographic and geochemical characteristics of the upper Aptian San Miguel de Allende volcanic sequence, located in central Mexico, are reported in this paper. This sequence may be the eastern remnant of an allocthonous volcanic stage in central Mexico and is a key element in understanding the petrologic evolution of the Guanajuato segment of the Guerrero terrane, and in constraining the time of emplacement of the arc series of the Mexican cordillera over the North America craton.

FIELD RELATIONSHIPS AND AGE OF THE SEQUENCE

The San Miguel de Allende volcanic sequence is situated in central Mexico, almost 50 km east of the city of Guanajuato, at the boundary between two physiographic provinces: the eastern edge of the Mexican Central Plateau and the northern edge of the Transmexican Volcanic Belt (Figure 1). This sequence was referred to as the Mesozoic basal rocks by Pérez-Vénzor *et al*. (1996), and is exposed south of the city of San Miguel de Allende (see Plate 1 from Pérez-Vénzor *et al*., 1996).

The San Miguel de Allende sequence forms a small 4 km^2 outcrop over 100 m thick. Its abrupt topography contrasts with the adjacent plain relief. The area is cut by the San Miguel de Allende-Cuernavaca fault system, which strikes N-S and the Chapala-Tula system fault with a N80°E strike. The sequence is made up of basalts and basaltic andesites, interbedded with graywacke containing lenticular, pelagic, fine-grained limestone, and also thin strata of black shale, radiolarite layers and epiclastic breccias. These rocks are in tectonic contact with flysch-type strata formed by sandstones and shales, limestones, and marls of probable Upper Cretaceous age (Figure 2). Limestones of the San Miguel de Allende sequence have amphibole and plagioclase debris, and undetermined bivalves and tests of planktonic Foraminifera determined as *Hedbergella* (Caron, verbal communication) that suggest a Cretaceous age *sensu lato*, after the biostratigraphic zonation of Longoria and Gamper (1975) and Longoria (1977). Nevertheless, the morphology of this fauna suggests a pre-Vraconian age (Caron, verbal communication), and a cold, epipelagic open-sea environment (Moullade, 1974). This age is confirmed by

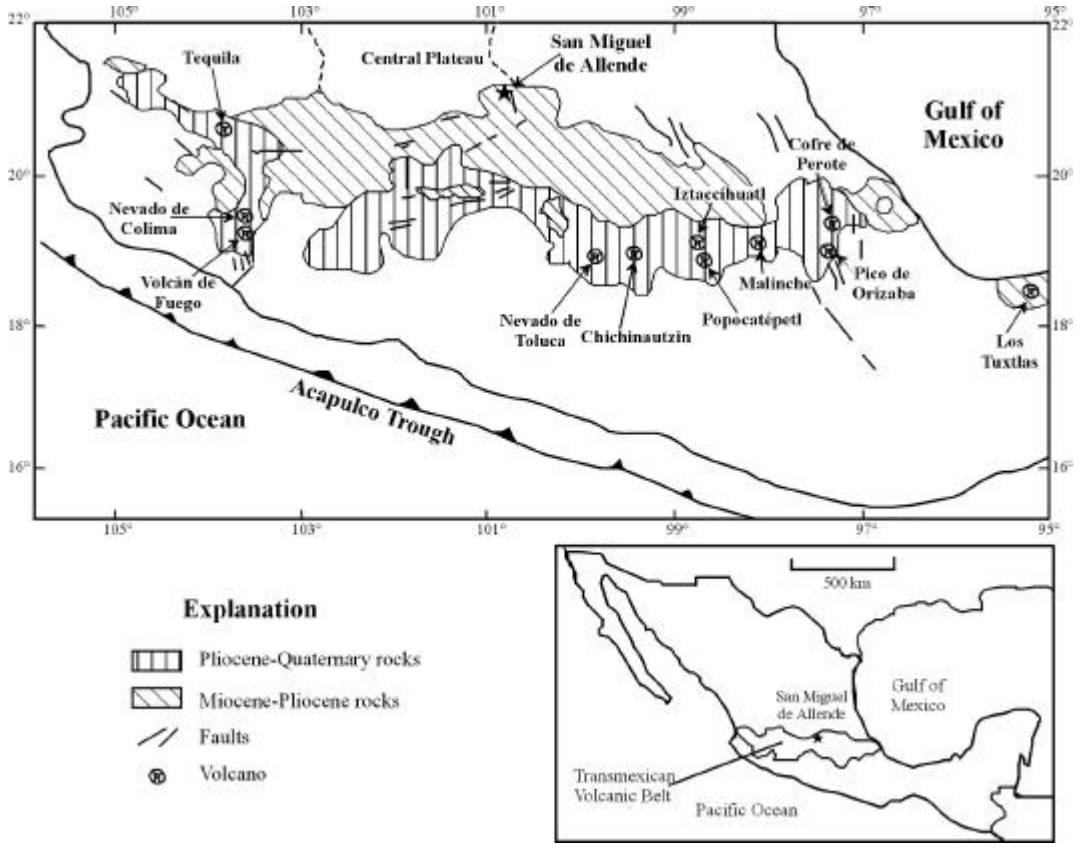

Figure 1. Location of the San Miguel de Allende sequence, situated north of the Transmexican Volcanic Belt (after Aguirre-Díaz, *et al*., 1997, modified).

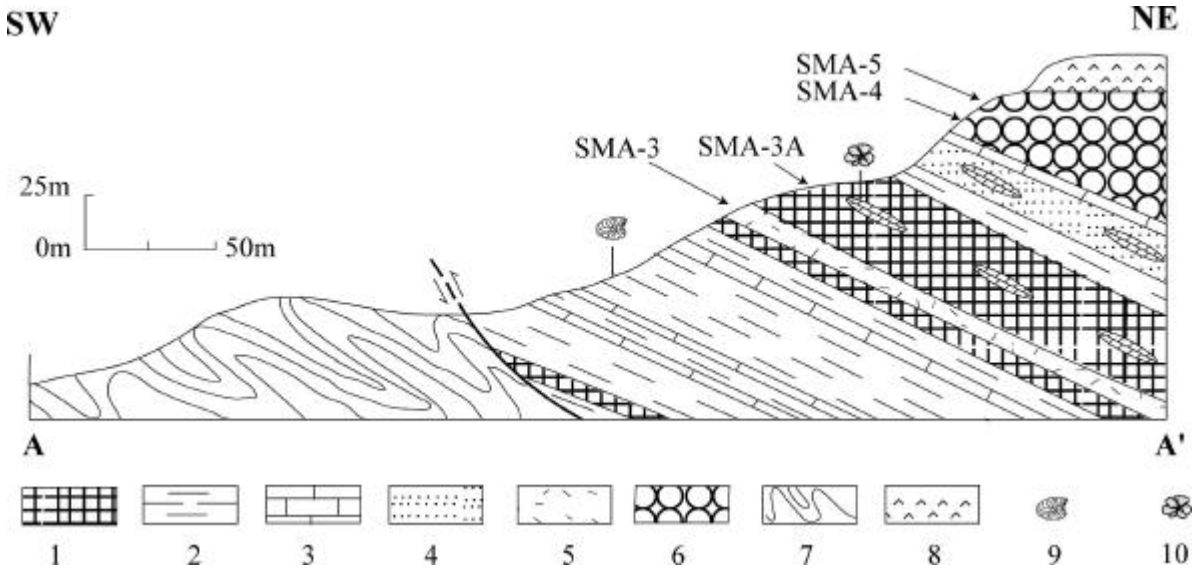

Figure 2. Geological cross-section of the San Miguel de Allende sequence showing location of the analyzed samples. 1: Graywacke; 2: shale; 3: pelagic limestone; 4: basic tuff; 5: massive basaltic lava; 6: basaltic and andesitic pillow lavas; 7: Upper (?) Cretaceous sandstone and shale; 8: Oligocene rhyolitic ignimbrite; 9: Ammonite fossils; 10: planktonic foraminifera.

the occurrence of ammonites (*Acanthohoplites sp.)* in black shales interbedded between two horizons of andesitic lavas (Chiodi *et al*., 1988), suggesting an upper Aptian age (Clansayesian) for this horizon.

No evidence of metamorphism is present in the San Miguel de Allende lavas. Nevertheless, in some places, they have been transformed into prasinites, which are formed by ouralitized sigmoid clinopyroxene crystals, saussuritized plagioclase crystals and acicular actinolite crystals showing a clear schistosity. The groundmass of these rocks is recrystallized to variable degrees, and consists of quartz and albite assemblages.

The graywackes and fine-grained breccias are mostly epiclastic and are derived from the erosion of volcanic rocks. They consist dominantly of small subangular debris of sericitized plagioclase, zoned clinopyroxene, microlitic, intersertal and trachytic-textured basalts, basic tuffs, orthopyroxenes transformed into smectite and chlorite aggregates, magnesio-hastingsitic amphiboles, recrystallized micritic limestones, dacites and siliceous sandstones with micritic cement. The debris is cemented either by micritic and argillaceous assemblages or by chlorite and clay mixtures.

Upper (?) Cretaceous rocks are formed from bottom to top by a succession of thin strata (1-2 cm thick) of gray to cream-colored limestone interbedded with shale. These rocks progressively turn into graywacke with laminar to thick stratification (1 cm to 1 m) interbedded with some conglomerate layers. There is cream-colored limestone interbedded with marls and laminations of gypsum at the top. Slump and convulate structures are common in the sequence, suggesting turbidite-related gravity flows.

The Middle Oligocene El Obraje rhyolitic ignimbrites dated at 28.6±0.7 Ma (K-Ar in sanidine; Nieto-Samaniego *et al*., 1996), dacites of the Cerro Colorado sequence (16.1±1.7 Ma; K-Ar in plagioclase; Pérez-Venzor *et al.*, 1996), the Allende andesite (11.1±0.4 Ma; K-Ar in whole-rock; Pérez-Venzor *et al.*, 1996), and volcanic and volcaniclastic rocks of the Palo Huérfano volcano (<11 Ma) unconformably overlie the Mesozoic rocks.

PETROGRAPHY AND MINERALOGY OF THE LAVAS

The minerals in the lavas were analyzed on a CAMEBAX microbeam electron microprobe at Joseph Fourier Grenoble University, France, using the matrix corrections of Hénoc and Tong (1978). Accelerating voltages of 15 kV and cup beam current of 10 ηA were used. All elements were counted for a maximum of 15 seconds. Standards were obtained from representative mineral compositions.

Basaltic lavas have both microlitic and porphyritic textures with euhedral to subhedral clinopyroxene phenocrysts and microphenocrysts (15%), ranging in composition from diopside ($Wo_{45.0\text{-}46.6}\,En_{49.2\text{-}51.1}\,Fs_{3.3\text{-}5.2}$) with high Mg numbers (91 < #Mg < 94) in the core to salite ($Wo_{45.2\text{-}47.8}\,En_{40.0\text{-}44.3}\,Fs_{10.5\text{-}13.0}$ and 77 < #Mg < 81) or calcic augite ($Wo_{42.5\text{-}44.9}\,En_{40.2\text{-}42.8}\,Fs_{12.5\text{-}16.8}$ and 72 < #Mg < 77) in the rim, as is shown in the conventional pyroxene quadrilateral (Figure 3 and Table 1). Scarce amphibole microphenocrysts, ranging in composition from hornblende magnesio-hastingsite to hornblende

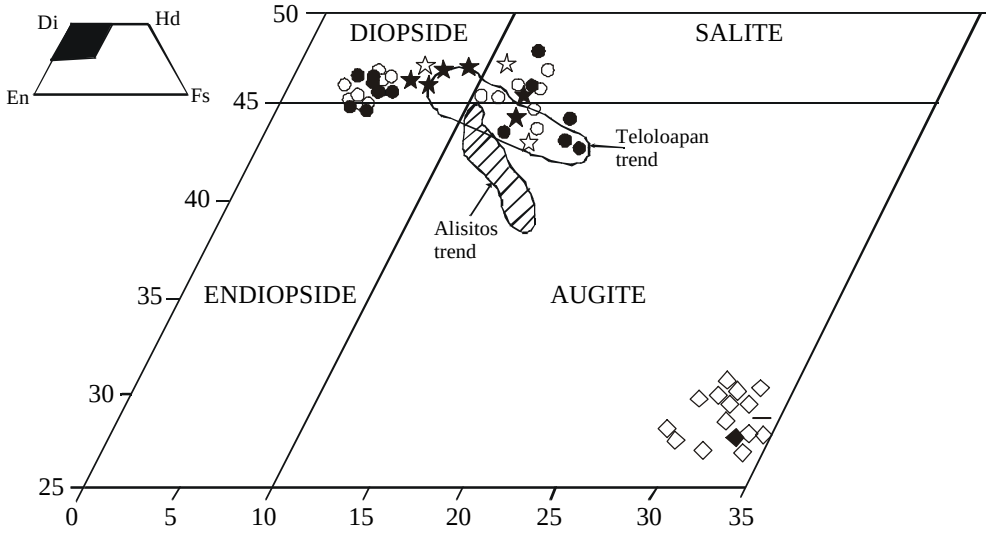

Figure 3. Pyroxene quadrilateral showing the clinopyroxene and amphibole composition. Full circle: clinopyroxene phenocryst core in basalt; open circle: clinopyroxene phenocryst rim in basalt; full star: clinopyroxene phenocryst core in basaltic andesite; open star: clinopyroxene phenocryst rim in basaltic andesite; full rhombus: amphibole microphenocryst in basalt; open rhombus: amphibole phenocryst in basaltic andesite.

hastingsite ($5.76 < Si < 6.27$ and $0.80 < Mg/Mg+Fe^{2+} < 0.89$) after the classification of the International Mineralogical Association (Leake *et al*., 1997; Figure 4 and Table 2), and labradorite microlites (Ab_{47-48}), are disseminated in the groundmass (Figure 5 and Table 3).

Basaltic andesites also have microlitic and porphyritic textures with subhedral phenocrysts of zoned clinopyroxene ranging from diopside ($Wo_{46.2-46.8}\ En_{44.1-46.9}\ Fs_{6.6-9.0}$ and $84 < \#Mg < 88$) to salite ($Wo_{45.7-47.5}\ En_{41.3-41.6}\ Fs_{11.2-12.7}$ and $77 < \#Mg < 79$) and scarce augite ($Wo_{43.4-44.5}\ En_{41.6-44.4}\ Fs_{11.4-13.9}$ and $76 < \#Mg < 80$) in the rim (Figure 3). Clinopyroxene also occurs as microphenocrysts with a composition of $Wo_{42.1-42.6}\ En_{41.5-42.9}\ Fs_{14.5-16.4}$ and $73 < \#Mg < 76$. Subhedral phenocrysts of sericitized plagioclase with normal zonation (core $Ab_{45}\ An_{53}\ Or_2$ and rim $Ab_{48}\ An_{50}\ Or_2$) or sieve textures with a labradorite core ($Ab_{44}\ An_{54}\ Or_2$), an external core of andesine ($Ab_{60}\ An_{33}\ Or_7$) and a rim of labradorite ($Ab_{45}\ An_{53}\ Or_2$) suggest magma mixing. Orthopyroxene relicts with apatite inclusions are completely transformed into smectite, chlorite, calcite and sphene aggregates in the core, and are replaced by actinolite in the rim. Sometimes, the orthopyroxene phenocrysts are surrounded by salitic clinopyroxene ($Wo_{45.6}\ En_{13.9}\ Fs_{40.5}$ and #Mg=75). Some augite phenocrysts are replaced by prismatic amphiboles with a hornblende magnesio-hastingsite composition ($5.78 < Si < 6.20$ and $0.77 < Mg/Mg+Fe^{2+} < 0.89$) and oxide rims (magnetite rims), suggesting disequilibrium between the phenocrysts and the rock groundmass or oxidation at low pressure. Scarce hornblende hastingsite (Si=6.33 and $Mg/Mg+Fe^{2+}=0.75$) crystals have small andesine inclusions ($Ab_{48}\ An_{49}\ Or_3$). The microlitic groundmass contains plagioclase with the composition $Ab_{45-51}\ An_{47-53}\ Or_{2-3}$ and secondary minerals such as chlorite and clays. In other cases, basaltic andesites have subangular, cogenetic inclusions of microlitic basalts with scarce pyroxene phenocrysts, and actinolite, chlorite and sphene in interstices.

Two trends in the compositional variation of both basaltic and basaltic andesites lavas are evident in quadrilateral pyroxene: (1) diopside to salite, and (2) diopside to calcic augite (Figure 3). Both the salitic and the augitic trends are characteristic of island arc lavas (Marcelot *et al*., 1988). The first one is marked by moderate enrichment in CaO, TiO_2 and greatly increased Al_2O_3, and high recalculated Fe_2O_3/FeO that suggest an early clinopyroxene-dominated fractionation in water-bearing melts, a hydration process due to an increase in P_{H2O} in the melt or a low silica content in the magma. Evidence of the last trend is shown by slight CaO depletion while Al_2O_3 and TiO_2 increase to constant levels. The augitic trend is interpreted as a low-pressure fractionation trend. Nevertheless, there is a reverse trend from augite cores to more magnesium augite rims that suggests a possible magma mixing process. The trend is closer to the Teloloapan calc-alkaline trend (Talavera-Mendoza *et al*., 1995) than to the Alisitos calc-alkaline trend (Almazán-Vázquez, 1988) (Figure 3). Amphiboles show a normal ferromagnesian trend in the pyroxene quadrilateral, evidenced by constant values of Fe and Mg in function of Ca (Figure 3), indicating $Mg \Leftrightarrow Fe^{2+}$ substitutions. Oxide amphibole rims around augitic clinopyroxene suggest an increase in both the water content and fO_2 in the magma during differentiation.

On the other hand, the "other" quadrilateral components (Papike *et al*., 1974) in the case of clinopyroxenes are mainly the Ca-Tschermak molecule ($CaAl_2SiO_6$) and in lesser proportion the molecules of Acmite-Jadeite-Ureyite ($AC=NaFeSi_2O_6$; $JD=NaAlSiO_6$; $UR=NaTiSiAlO_6$), that suggest the presence of two cli-

Table 1. Microprobe analyses of clinopyroxene phenocrysts (wt %) from basalt (sample SMA-3, analyses 1 to 15) and basaltic andesites (samples SMA-4 and SMA-5, analyses 16 to 29) from San Miguel de Allende sequence (c: core; r: rim).

	1	**2**	**3**	**4**	**5**	**6**	**7**	**8**	**9**	**10**	**11**	**12**	**13**	**14**	**15**
	c	**c**	**c**	**c**	**c**	**c**	**c**	**r**	**r**	**r**	**r**	**r**	**r**	**r**	**c**
SiO_2	54.57	55.46	55.13	54.93	55.20	55.15	55.20	54.46	54.65	55.03	55.17	55.12	54.48	54.88	50.51
TiO_2	0.13	0.12	0.09	0.16	0.09	0.14	0.18	0.20	0.08	0.19	0.15	0.09	0.07	0.12	0.78
Al_2O_3	0.84	0.74	0.59	0.86	0.90	0.81	0.98	0.95	0.74	0.97	0.92	0.77	0.72	0.86	4.88
FeO	2.48	2.33	2.52	2.62	3.15	2.96	2.66	3.09	2.58	2.92	2.71	2.11	2.59	2.52	7.55
Cr_2O_3	0.55	0.52	0.37	0.23	0.56	0.54	0.54	0.27	0.47	0.29	0.11	0.41	0.62	0.53	0.02
MnO	0.07	0.15	0.10	0.06	0.14	0.16	-	-	0.20	0.18	0.07	0.01	0.17	0.02	0.20
MgO	18.26	18.31	18.40	17.88	17.34	17.65	17.42	17.68	17.98	17.66	17.48	18.14	18.14	18.16	13.89
CaO	22.74	22.48	23.06	23.22	22.57	22.79	22.97	23.15	22.42	22.69	22.92	22.97	22.49	22.54	21.50
Na_2O	0.07	0.21	0.03	0.16	0.22	0.15	0.09	0.08	0.20	0.06	0.15	0.12	0.18	0.19	0.42
TOTAL	99.71	100.32	100.29	100.12	100.17	100.35	100.04	99.8	99.32	99.99	99.68	99.74	99.46	99.82	99.75
Si	1.981	1.996	1.990	1.988	1.998	1.993	1.996	1.980	1.992	1.993	2.001	1.995	1.985	1.988	1.877
Ti	0.004	0.003	0.002	0.004	0.002	0.004	0.005	0.005	0.002	0.005	0.004	0.002	0.002	0.003	0.022
Al	0.036	0.031	0.025	0.037	0.038	0.034	0.042	0.041	0.032	0.041	0.039	0.033	0.031	0.037	0.214
Fe^{2+}	0.075	0.07	0.076	0.079	0.095	0.089	0.080	0.094	0.079	0.088	0.082	0.064	0.079	0.076	0.235
Cr	0.016	0.015	0.011	0.007	0.016	0.015	0.015	0.008	0.014	0.008	0.003	0.012	0.018	0.015	0.001
Mn	0.005	0.005	0.003	0.002	0.004	0.005	-	-	0.006	0.006	0.002	-	0.005	0.001	0.006
Mg	0.990	0.982	0.990	0.964	0.935	0.951	0.939	0.958	0.977	0.953	0.945	0.979	0.985	0.981	0.769
Ca	0.885	0.867	0.892	0.900	0.875	0.882	0.890	0.902	0.876	0.880	0.891	0.891	0.878	0.875	0.856
Na	0.0005	0.015	0.002	0.011	0.015	0.011	0.006	0.006	0.014	0.004	0.011	0.008	0.013	0.013	0.030
TOTAL	3.997	3.984	3.991	3.992	3.978	3.984	3.973	3.994	3.992	3.978	3.978	3.984	3.996	3.989	4.010
% En	50.7	51.1	50.5	49.6	49	49.3	49.2	49.0	50.4	49.5	49.2	50.6	50.6	50.7	41.2
% Fs	4.0	3.9	4.0	4.2	5.2	4.9	4.2	4.8	4.4	4.9	4.4	3.3	4.3	4.0	12.9
% Wo	45.3	45	45.5	46.2	45.8	45.8	46.6	46.2	45.2	45.6	46.4	46.1	45.1	45.3	45.9
Al^{IV}	0.019	0.004	0.010	0.012	0.002	0.007	0.004	0.020	0.008	0.007	-	0.005	0.015	0.012	0.123
Al^{VI}	0.017	0.027	0.015	0.025	0.036	0.027	0.038	0.020	0.024	0.034	0.039	0.028	0.016	0.025	0.091
# Mg	88	89	88	87	85	86	87	85	87	86	87	90	88	88	65

	16	**17**	**18**	**19**	**20**	**21**	**22**	**23**	**24**	**25**	**26**	**27**	**28**	**29**
	c	**c**	**c**	**c**	**r**	**r**	**c**	**c**	**c**	**c**	**c**	**r**	**r**	**r**
SiO_2	51.43	49.91	51.60	52.17	52.38	51.24	50.89	50.65	49.38	52.00	52.60	49.1	50.88	53.68
TiO_2	0.36	0.69	0.27	0.19	0.19	0.58	0.45	0.55	0.77	0.41	0.19	0.75	0.42	0.16
Al_2O_3	1.58	4.26	2.57	1.95	1.91	2.90	2.98	3.84	4.67	2.38	1.69	4.95	2.91	1.12
FeO	9.78	7.59	5.50	4.43	4.43	8.20	6.10	8.22	7.45	8.54	4.87	6.78	6.88	4.11
Cr_2O_3	-	0.07	0.15	0.38	0.37	-	0.16	-	0.17	0.08	0.43	-	0.14	0.18
MnO	0.48	0.20	0.17	0.10	0.03	0.19	0.21	0.28	0.27	0.41	0.05	0.14	0.25	0.18
MgO	14.54	14.27	15.55	16.68	16.44	14.88	15.82	14.22	14.75	14.88	16.53	14.26	15.64	17.00
CaO	20.54	21.79	22.97	22.93	23.2	20.92	22.22	21.17	21.40	20.54	23.29	22.85	21.72	23.44
Na_2O	0.33	0.26	0.24	0.18	0.23	0.28	0.24	0.35	0.24	0.32	0.17	0.24	0.22	0.13
TOTAL	99.04	99.04	99.02	99.01	99.18	99.19	99.07	99.28	99.10	99.56	99.82	99.07	99.06	100.00
Si	1.943	1.873	1.922	1.933	1.938	1.917	1.899	1.896	1.352	1.939	1.938	1.843	1.902	1.964
Ti	0.010	0.019	0.008	0.005	0.005	0.016	0.013	0.015	0.022	0.011	0.005	0.021	0.012	0.004
Al	0.070	0.188	0.113	0.085	0.083	0.128	0.131	0.169	0.206	0.105	0.073	0.219	0.128	0.048
Fe^{2+}	0.309	0.238	0.171	0.137	0.137	0.257	0.190	0.257	0.234	0.266	0.150	0.213	0.215	0.126
Cr	-	0.002	0.004	0.011	0.011	-	0.005	-	0.005	0.002	0.013	0.000	0.004	0.005
Mn	0.015	0.006	0.003	0.003	0.001	0.006	0.007	0.009	0.009	0.013	0.002	0.004	0.008	0.006
Mg	0.819	0.798	0.863	0.921	0.907	0.830	0.880	0.794	0.825	0.827	0.908	0.798	0.872	0.927
Ca	0.832	0.876	0.917	0.910	0.920	0.839	0.888	0.849	0.860	0.821	0.919	0.919	0.870	0.919
Na	0.024	0.019	0.017	0.013	0.016	0.020	0 0.017	0.025	0.017	0.023	0.012	0.017	0.016	0.009
TOTAL	4.022	4.019	4.018	4.020	4.018	4.013	4.03	4.014	4.030	4.007	4.020	4.034	4.027	4.008
% En	41.5	41.6	44.0	46.7	46.2	43	44.8	41.6	42.8	42.9	45.8	41.3	44.3	46.9
% Fs	16.4	12.7	9.1	7.1	7.0	13.6	10.0	13.9	12.6	14.5	7.7	11.2	11.4	6.6
% Wo	42.1	45.7	46.8	46.2	46.8	43.4	45.2	44.5	44.6	42.6	46.5	47.5	44.3	46.5
Al^{IV}	0.057	0.127	0.078	0.067	0.062	0.083	0.101	0.104	0.148	0.061	0.062	0.157	0.098	0.036
Al^{VI}	0.014	0.062	0.035	0.018	0.021	0.045	0.03	0.066	0.058	0.044	0.011	0.062	0.031	0.013
# Mg	60	65	86	79	79	64	72	63	66	64	77	68	69	81

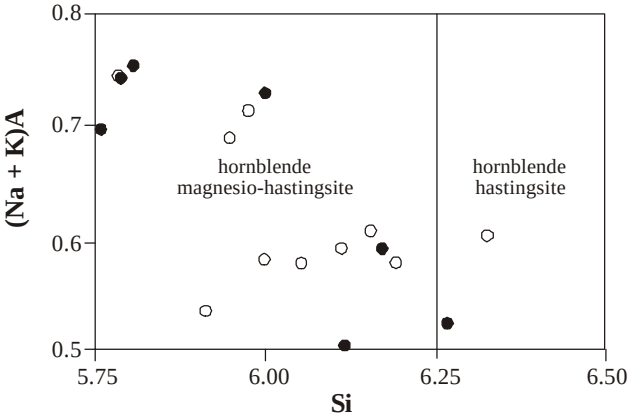

Figure 4. Si-$(Na+K)_A$ diagram (after Leake *et al*., 1997) showing the amphibole composition. Full circle: amphibole microphenocryst in basalt; open circle: amphibole phenocryst in basaltic andesite.

nopyroxene populations: the first one probably crystallizing at higher pressure (diopside) than the second (augite-salite), which is corroborated by their contrasting Al/Ti ratios. Silica undersaturated liquids favour incorporation of larger amounts of the Ca-Tschermak molecule in pyroxenes whereas the AC-JD-UR substitutions suggest the role of variable pressure and oxygen fugacity prevailing over these crystallizing phases during magmatic differentiation.

"Other" quadrilateral components for the amphiboles are the Pargasite-Hastingsite-Kaersutite molecules ($NaCa_2Mg_4Fe_4^{2+}Fe^{3+}Si_6Al_2$) that suggest the role of the bulk rock composition and the change in the pressure and fugacity prevailing at the time of crystallization of these ferromagnesian minerals.

According to Semet and Ernst (1981), hastingsitic amphibole is stable over a wide range of P, T, and fO_2, but is characteristic of upper crustal rocks crystallizing at relatively low oxygen fugacity (Thomas, 1982). The presence of Mg, K, and F in small amounts expands their stability field under higher fO_2 values. The incipient melting of a fluid-modified upper mantle may leave magnesio-hastingsite amphibole as a refractory residual phase (Semet and Ernst, 1981).

CHEMICAL COMPOSITION

Three analyses of the lavas were performed by X-ray fluorescence spectrometry for major elements (expressed in weight %) and for trace elements, including rare earth elements (expressed in ppm), by ICP-

Table 2. Microprobe analyses (wt %) of amphibole microphenocrysts in basalt (sample SMA-3, analyses 1 to 7) and amphibole phenocrysts in basaltic andesites (samples SMA-4 and SMA-5, analyses 8 to 18). Table 2. Microprobe analyses (wt %) of amphibole microphenocrysts in basalt (sample SMA-3, analyses 1 to 7) and amphibole phenocrysts in basaltic andesites (samples SMA-4 and SMA-5, analyses 8 to 18). Structural formulae calculated using the method of Robinson *et al*. (1982). Fe partition calculated using the charge balance equation of Papike *et al*. (1974).

	1	**2**	**3**	**4**	**5**	**6**	**7**	**8**	**9**	**10**	**11**	**12**	**13**	**14**	**15**	**16**	**17**	**18**
SiO_2	39.53	39.69	39.83	43.04	42.54	43.51	41.09	42.55	42.6	41.6	41.33	39.05	41.00	39.98	40.36	40.48	40.74	41.67
TiO_2	1.82	1.80	1.93	2.41	1.47	2.77	1.70	3.00	2.69	2.85	2.31	1.84	2.22	2.99	2.05	2.04	2.18	3.02
Al_2O_3	15.21	15.8	15.03	11.79	12.75	10.85	13.98	10.38	10.1	11.1	11.09	13.95	11.56	11.89	13.39	13.22	13.27	10.71
FeO	10.92	11.00	11.96	10.36	10.19	10.95	10.32	11.92	12.91	11.52	11.92	11.2	11.48	12.25	11.22	11.01	11.18	12.52
Cr_2O_3	0.04	0.09	0.11	-	0.08	-	0.13	-	-	-	-	0.06	0.02	0.10	0.03	-	0.09	-
MnO	0.14	0.06	0.09	0.05	0.04	0.32	0.18	0.20	0.22	0.28	0.28	0.28	0.15	0.15	-	0.13	0.15	0.18
MgO	13.87	13.85	13.41	15.56	15.52	15.07	14.31	13.55	13.4	14.21	14.47	14.24	14.79	14.25	13.93	14.29	13.89	13.61
CaO	12.00	11.93	12.04	11.17	11.27	10.82	11.83	11.1	10.84	11.10	11.18	12.12	11.63	11.10	12.12	11.97	11.57	11.07
Na_2O	2.27	2.26	2.35	2.58	2.31	2.45	2.54	2.42	2.55	2.55	2.55	2.46	2.16	2.29	2.39	2.44	2.29	2.45
K_20	1.16	1.12	1.12	0.87	0.65	0.93	0.86	0.72	0.77	0.62	0.49	0.60	0.65	0.65	0.57	0.55	0.55	0.59
Total	96.96	97.60	97.87	97.83	96.82	97.67	96.94	95.84	96.08	95.83	95.32	95.80	95.66	95.65	96.06	96.13	95.91	95.82
Si	5.788	5.756	5.807	6.172	6.115	6.265	5.997	6.330	6.330	6.153	6.111	5.784	6.051	5.910	5.972	5.946	5.999	6.192
Ti	0.200	0.196	0.212	0.260	0.159	0.300	0.187	0.336	0.301	0.317	0.257	0.205	0.246	0.332	0.228	0.226	0.241	0.338
Al^{IV}	2.212	2.244	2.193	1.828	1.885	1.735	2.003	1.670	1.670	1.847	1.889	2.216	1.949	2.072	2.028	2.036	2.001	1.808
Al^{VI}	0.413	0.458	0.391	0.165	0.276	0.107	0.403	0.151	0.099	0.089	0.045	0.221	0.062	-	0.308	0.263	0.303	0.069
Fe^{2+}	0.571	0.502	0.729	0.410	0.179	0.486	0.628	1.010	0.968	0.670	0.511	0.478	0.973	0.380	0.765	0.616	0.582	0.836
Fe^{3+}	0.767	0.832	0.730	0.833	1.046	0.833	0.632	0.473	0.637	0.755	0.964	0.909	0.973	1.117	0.624	0.741	0.795	0.72
Cr	0.005	0.010	0.013	-	0.009	-	0.015	-	-	-	-	0.007	0.002	0.012	0.004	-	0.010	-
Mn	0.017	0.007	0.011	0.006	0.005	0.039	0.022	0.025	0.026	0.035	0.035	0.035	0.019	0.019	-	0.016	0.019	0.023
Mg	3.027	2.994	2.914	3.326	3.326	3.235	3.113	3.005	2.968	3.133	3.189	3.144	3.253	3.140	3.072	3.138	3.049	3.015
Ca	1.883	1.854	1.881	1.717	1.736	1.670	1.850	1.770	1.726	1.760	1.772	1.924	1.839	1.758	1.922	1.89	1.826	1.763
Na	0.644	0.636	0.665	0.717	0.644	0.684	0.719	0.698	0.735	0.731	0.731	0.707	0.618	0.657	0.686	0.697	0.654	0.706
K	0.217	0.207	0.208	0.159	0.120	0.171	0.16	0.137	0.146	0.117	0.092	0.113	0.122	0.123	0.108	0.103	0.103	0.112
NaB	0.117	0.146	0.119	0.283	0.264	0.330	0.15	0.230	0.274	0.240	0.228	0.076	0.161	0.242	0.078	0.110	0.174	0.237

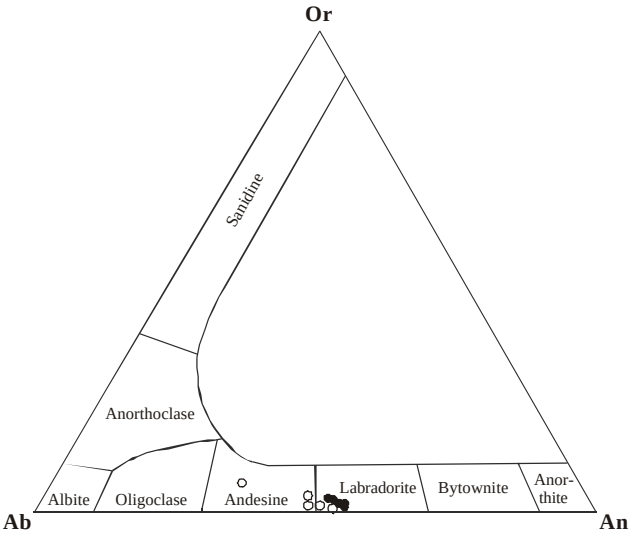

Figure 5. Ab-An-Or ternary plot showing the plagioclase composition for the lavas. Full circle: phenocryst in basalt; open circle: phenocryst in basaltic andesite.

Atomic Emission Spectrometry. All analyses were carried out at the *Centre des Recherches Pétrographiques et Géochimiques* of Nancy, France, following the analytical procedures of Govindaraju and Mevell (1987). Accuracy of analysis is 1% for major elements and 2% for trace elements. Loss on ignition (LOI) was performed at 900 ° C in a muffle furnace.

The basalt sample analyzed (SMA-3) is depleted in SiO_2, TiO_2, Al_2O_3 and alkalis, and rich in Fe_2O_3, CaO and MgO (Table 4), suggesting a primitive nature that is corroborated by high values for the transition elements (Cr and Ni), and by their Mg number [(100Mg/(Mg+Fe*)] = 45. The basalt is enriched in Sr (637 ppm) but depleted in Ba (204 ppm) and Rb (16 ppm) compared to mean values reported for typical calc-alkaline basalts (Sr=428 ppm, Ba=260 ppm, and Rb=23 ppm). Their Ti/V ratio is equal to 17, which is characteristic of volcanic rocks from modern island arcs. Their Nb content (20 ppm) is high compared to island arc basalts, but this is a geochemical characteristic of basic lavas from the Guanajuato segment of the Guerrero terrane (Lapierre *et al*., 1992). This Nb-enrichment has been reported from Nb-enriched basalts associated with adakitic lavas (Nb = 15-17 ppm).

Island arc basalts (IAB) have variable concentrations of Al_2O_3 (13-18 wt%), TiO_2 < 1.2 wt% and total FeO ranging from 6 to 15 wt% (Perfit *et al*., 1980). IAB are distinguished from other basalt types by their high V/Ni and V/Cr ratios and also the absolute abundance of LILE, and their chondrite-normalized REE patterns, that vary from relatively flat (La/Yb ~1) in low-K basalts to light-REE enriched (La_{ch} = 20-100; Yb_{ch}= 6-30) in moderate to high-K basalts (Perfit *et al.*, 1980).

Basaltic andesites (samples SMA-4 and SMA-5) are depleted in SiO_2, TiO_2, Fe_2O_3 and MgO (Mg number ranging from 36 to 41), but they are moderately rich in Al_2O_3 and K_2O (K_2O < 2 wt%) (Table 4). Trace element concentrations are typical of volcanic rocks from recent island arcs, and are characterized by a relatively high LILE content and a depletion of highly charged incompatible elements (Dixon and Batiza, 1979; Bailey, 1981). According to Bailey (1981), the geochemical characteristics of orogenic andesites are: high Al_2O_3 values (generally >15.5 wt%, often >17wt%), low FeO* (5-8.5 wt%), TiO_2 (0.5-1.3 wt%), Zr (35-250 ppm), Y (8-40 ppm), and Nb (0.3-21 ppm) values. Low Ga/Sc (< 1.5)

Table 3. Microprobe analyses of plagioclase phenocrysts (wt %) from basalt (sample SMA-3, analyses 1 and 2) and basaltic andesites (samples SMA-4 and SMA-5, analyses 3 to 10).

	1	2	3	4	5	6	7	8	9	10
SiO_2	55.41	55.11	54.47	54.78	55.38	54.3	54.11	59.37	53.97	54.11
Al_2O_3	28.22	27.43	28.27	27.91	27.2	27.78	28.38	24.52	28.37	28.12
FeO	0.87	0.67	0.4	0.49	0.48	0.66	0.4	0.9	0.45	0.54
CaO	10.54	10.19	10.75	10.24	9.79	10.48	10.95	6.55	10.98	10.88
Na_2O	5.31	5.35	5	5.33	5.81	5.62	4.91	6.65	5.25	5.05
K_20	0.42	0.39	0.38	0.37	0.36	0.5	0.29	1.05	0.2	0.33
TOTAL	100.77	99.14	99.27	99.12	99.02	99.34	99.04	99.04	99.22	99.03
Si	2.488	2.51	2.478	2.49	2.52	2.48	2.47	2.684	2.46	2.47
Al	1.494	1.473	1.516	1.5	1.46	1.5	1.53	1.306	1.525	1.51
Fe	0.033	0.026	0.015	0.019	0.018	0.025	0.015	0.034	0.017	0.02
Ca	0.507	0.497	0.524	0.5	0.48	0.513	0.54	0.32	0.54	0.53
Na	0.462	0.473	0.441	0.471	0.51	0.5	0.43	0.058	0.46	0.45
K	0.024	0.023	0.022	0.022	0.02	0.029	0.017	0.06	0.012	0.019
TOTAL	5.008	5.002	4.996	5.002	5.008	5.047	5.002	4.99	5.014	4.999
% An	51	50.1	53.08	50.38	47.22	49.33	54.26	33.02	53	53.3
% Ab	46.5	47.6	44.68	47.45	50.71	47.87	44.02	60.66	45.85	44.77
% Or	2.5	2.3	2.24	2.17	2.07	2.8	1.72	6.32	1.15	1.93

Table 4. Chemical analyses for basaltic (sample SMA-3) and andesitic lavas (samples SMA-4 and SMA-5). Major elements in wt % and trace elements in ppm.

	SMA-3	SMA-4	SMA-5
SiO_2	47.04	53.95	54.42
TiO_2	0.65	0.68	0.65
Al_2O_3	14.21	18.35	18.07
Fe_2O_3	10.71	6.44	6.55
MnO	0.20	0.08	0.08
MgO	8.16	3.52	3.54
CaO	11.69	7.15	6.75
Na_2O	2.09	4.41	4.34
K_2O	0.98	1.66	1.62
P_2O_5	0.32	0.32	0.30
LOI	4.00	3.21	3.38
TOTAL	100.05	99.77	99.70
Rb	16	24	25
Sr	637	731	702
Ba	204	253	238
Cr	466	42	38
Ni	76	24	24
V	223	183	177
Zr	19	99	95
Y	15	17	17
Nb	20	5	5
La	7.04	10.50	10.48
Ce	19.74	23.31	24.42
Nd	11.06	14.34	15.04
Sm	2.94	3.67	3.71
Eu	0.91	1.11	1.12
Gd	2.81	3.33	3.50
Dy	2.37	2.82	2.81
Er	1.20	1.63	1.68
Yb	1.18	1.69	1.71
Lu	0.32	0.29	0.29
(La/Yb)N	4.03	4.19	4.14

ratios, (35 ppm < ΣREE < 74 ppm) and the absence of pronounced negative Eu anomalies (Eu/Eu* > 0.75) are also characteristic. The San Miguel de Allende basaltic andesites are similar to andesites of oceanic island arcs. The slightly Y enrichment in these lavas is probably due to the presence of amphibole in the mantle source, as occurs in the calc-alkaline lavas from the northern Mariana arc (Dixon and Batiza, 1979).

The chondrite-normalized REE patterns of the San Miguel de Allende lavas have a slight LREE enrichment with $(La/Yb)_N = 4$ (normalizing values of Evensen *et al*., 1978; Figure 6), suggesting a low degree of fractionation for these rocks. This is corroborated by their total REE content, which is relatively low (49 ppm for the basalt and ranging from 62 ppm to 64 ppm for the basaltic andesites). Small negative Eu anomalies indicative of plagioclase fractionation are seen in the lava patterns, with Eu/Eu* ranging from 0.93 to 0.95.

Multielemental diagrams show a distinctive large

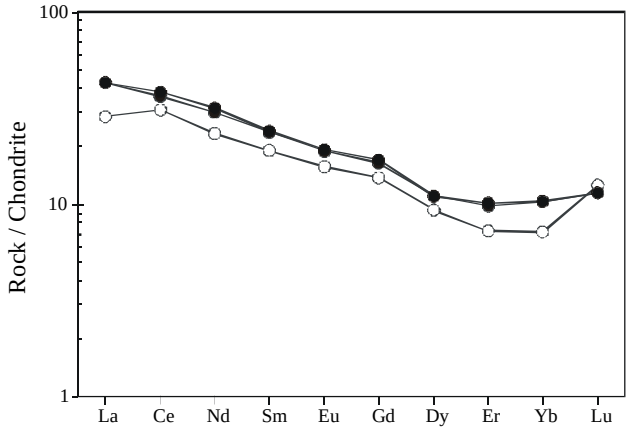

Figure 6. Chondrite-normalized REE patterns for the San Miguel de Allende lavas. Normalization values of Evensen *et al*. (1978). Open circle: basalt; full circle: basaltic andesites.

ion lithophile element (LILE) enrichment and a depletion in high-field strength elements (HFSE) (Figure 7) compared to normal MORBs, which is characteristic of lavas erupted in subduction settings (Pearce, 1983). The San Miguel de Allende basalt and basaltic andesites have geochemical characteristics of medium-K calc-alkaline island arc lavas.

DISCUSSION

The Upper Jurassic-Early Cretaceous arc-lavas from central Mexico, exposed in the Sierra de Guanajuato and in Zacatecas state are mainly LREE-depleted tholeiitic basalts, and slightly LREE-enriched tholeiitic and calc-alkaline basalts (Ortiz-Hernández *et al*., 1991b). They are interbedded with pelagic and volcaniclastic sediments that resemble deposits from an open-sea environment.

On the other hand, the San Miguel de Allende volcanic rocks consist of slightly LREE-enriched basalts and basaltic andesites belonging to a medium-K calc-alkaline suite. Petrographically they are classified as clinopyroxene±amphibole basalts and two-pyroxene ± amphibole basaltic andesites. They are interbedded with pelagic limestones, black shales, radiolarites, and epiclastic rocks, that are in tectonic contact with Upper (?) Cretaceous flysch-like strata. They represent a more evolved volcanic stage compared to the LREE-depleted tholeiitic rocks present in Sierra de Guanajuato and Zacatecas state.

These characteristics suggest that during the upper Aptian, the calc-alkaline rocks were extruded in an intra-arc environment that coincided in time and space with tholeiitic volcanism. Their eastern emplacement is possibly due to the tectonic transport (thrusting) of the arc over the North America craton during Early Cretaceous time.

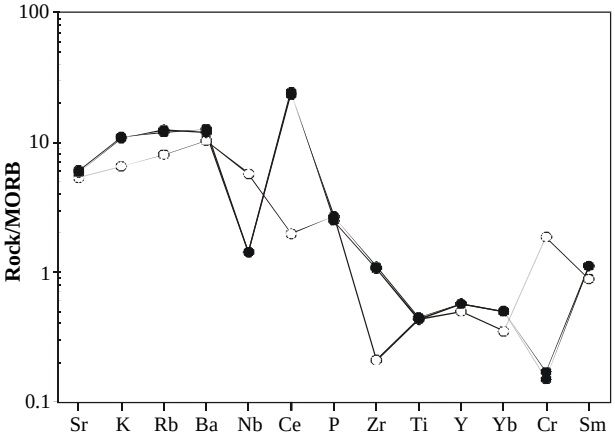

Figure 7. Multielemental diagrams normalized to MORB (Pearce, 1983) for the San Miguel de Allende lavas. Open circle: basalt; full circle: basaltic andesites.

These calc-alkaline series lavas from San Miguel de Allende probably were derived by low degrees of partial melting of mantle sources similar to those that produced tholeiitic arc lavas. Nevertheless, the San Miguel de Allende calc-alkaline volcanism represents hydrous partial melts of depleted hot Pacific plate lithosphere that had been enriched by both LILE and LREE from a mantle or subducted slab derived fluid. Migrating hydrous fluids released during the dehydration of the subducted oceanic lithosphere probably produced the LILE enrichment. Such a source is probably very refractory, and it would require special conditions as well as high H_2O contents and relatively low pressures (6-10 kb) at 1000 to 1100° C.

The petrologic evolution of the Guanajuato segment of the Guerrero terrane is thus similar to other intra-oceanic island arcs (Aleutian arc or Mariana arc, for example), where both tholeiitic and calc-alkaline basaltic and basaltic andesites are the predominant lava types. Transitional tholeiitic and calc-alkaline lavas may occur (Kay and Kay, 1985).

In this context, the upper Aptian San Miguel de Allende volcanic sequence represents the eastern remnant of an allochthonous Lower Cretaceous volcanic stage. This is contemporaneous with other volcanosedimentary sequences exposed in northwestern (Alisitos Formation; Almazán-Vázquez, 1988) and central Mexico (Teloloapan assemblage; Talavera-Mendoza *et al*., 1995).

According to Tardy and Maury (1973), reworked material found in the Upper Cretaceous flysches in northeastern-central Mexico is calc-alkaline and andesitic, dacitic, and rhyolitic in composition. The basalts and basaltic andesites of the San Miguel de Allende sequence are possibly part of a diversified calc-alkaline magmatic series, located to the west of the Valles-San Luis Potosí carbonate platform.

ACKNOWLEDGMENTS

The first author is indebted to CONACYT for its financial support. We want to express our appreciation to Henriette Lapierre from Joseph Fourier Grenoble University for the chemical analyses. We also wish to thank Elena Centeno García for valuable comments that improved the manuscript, and Barbara Martiny for improving the English.

REFERENCES

Aguirre-Díaz, G.J., Aranda-Gómez, J.J., Carrasco-Núñez, G., Ferrari, L. (eds.), 1997, Magmatism and tectonics of central and northwestern Mexico-a selection of the 1997 IAVCEI General Assembly Excursions: México, Universidad Nacional Autónoma de México, Instituto de Geología, 151 p.

Almazán-Vázquez, E., 1988, Geoquímica de las rocas volcánicas de la Formación Alisitos del arroyo La Bocana en el estado de Baja California Norte: México, Universidad Nacional Autónoma de México, Instituto de Geología, Revista, 7, 78-88.

Bailey, J.C., 1981, Geochemical criteria for a refined tectonic discrimination of orogenic andesites: Chemical Geology, 32, 139-154.

Centeno-García, E., 1994, Tectonic evolution of the Guerrero terrane, western Mexico: Tucson, Arizona, University of Arizona, Ph. D. Thesis, 220 p. (unpublished).

Chiodi, M., Gaspard, D., Sánchez, A., Yta, M., Monod, O., Busnardo, R., 1988, Une discordance anté-albienne datée par une faune d´ammonites et de brachiopodes de type théthysien au Mexique central: Geobios, 211, 125-135.

de Cserna, Z., 1976, Geology of the Fresnillo area, Zacatecas, Mexico: Geological Society of America Bulletin, 87, 1191-1199.

Dixon, T.H., Batiza, R., 1979, Petrology and chemistry of recent lavas in the northern Marianas: implications for the origin of island arc basalts: Contributions to Mineralogy and Petrology, 70, 167-181.

Evensen, N.M., Hamilton, P.J., O´Nions, R.K., 1978, Rare-earth abundances in chondritic meteorites: Geochimica and Cosmochimica Acta, 42, 1999-1212.

Freydier, C., Tardy, M., Martínez-Reyes, J., Coulon, Ch., Lapierre, H., Ruiz, J., 2000, The Early Cretaceous Arperos basin; an oceanic domain dividing the Guerrero arc from nuclear Mexico evidenced by the geochemistry of the lavas and sediments, *in* Centeno-García, E., Lomnitz, C., Ramírez-Espinoza, J. (eds.), Special issue geological evolution of the Guerrero terrane, western Mexico: Journal of South American Earth Sciences, 13, 325-336.

Govindaraju, K., Mevell, G., 1987, Fully automated dissolution and separation methods for inductively coupled plasma atomic emission spectrometry rocks analysis. Application to the determination of rare earth elements: Journal of Analytical and Atomic Spectrometry, 2, 615-621.

Hénoc, J., Tong, M., 1978, Automatisation de la microsonde: Journal de Microscopie et de Spectrometrie Electroniques, 2, 247-254.

Kay, S.M., Kay, R.W., 1985, Aleutian tholeiitic and calc-alkaline magma series I: The mafic phenocrysts: Contribution to Mineralogy and Petrology, 90, 276-290.

Lapierre, H., Ortiz-Hernández, E., Abouchami W., Monod O., Coulon, Ch., Zimmermann J. L., 1992, A crustal section of an intraoceanic island arc; the late Jurassic-early Cretaceous Guanajuato magmatic sequence (central Mexico): Earth and Planetary Science Letters, 108, 61-77.

Leake, B.E., Gilbert, M.Ch., Grice, J.D., Hawthorne, F.C., Kato, A., Kisch, H.J., Krivovichev, V.G., Linthout, K., Laird, J., Mandarino, J.A., Maresch, W.V., Nickel, E.H., Rock, N.M.S., Schumacher, J.C., Smith, D.C.., Stephenson, N.C.N., Ungaretti, L., Whittaker, E.J.W., Youzhi, G., Wooley, A.R., Arps, Ch. E.S., Birch, W. D., 1997, Nomenclature of amphiboles:

report of the Subcommittee on amphiboles of the International Mineralogical Association, Commission on New Minerals and Mineral Names: The Canadian Mineralogist, 35, 219-246.

Longoria, J.F., Gamper, M.A., 1975, The classification and evolution of Cretaceous planktonic Foraminifera. Part 1: The superfamily Hedbergelloidea: Revista Española de Micropaleontología, 7, 61-96.

Longoria, J.F., 1977, El límite Cretácico Inferior-Cretácico Superior en México basado en los foraminíferos planctónicos: México, Universidad Nacional Autónoma de México, Instituto de Geología, Revista, 1 (1), 10-22.

Marcelot, G., Bardintzeff, J.M., Maury, R. C., Rançon, J.Ph., 1988, Chemical trends of early-formed clinopyroxene phenocrysts from some alkaline and orogenic basic lavas: Bulletin de la Société Géologique de France, Huitième serie, 4, 851-859.

Monod, O., Lapierre, H., Chiodi, M., Martínez, J. Calvet, Ph., Ortiz, E., Zimmermann, J.L., 1990, Reconstitution d´un arc insulaire intra-océanique au Mexique central: la séquence volcano-plutonique de Guanajuato (Crétacé inférieur): Comptes Rendus de l´Académie des Sciences, Serie II, 310 (4), 45-51.

Moullade, M., 1974, Zones des Foraminifères du Crétacé inférieur mésogéen: Comptes Rendus Hebdomaires des Seances de l´Académie des Sciences, Serie D, Sciences Naturelles, 278 (14), 1813-1816.

Nieto-Samaniego, A.F., Macías-Romo, C., Alaniz-Álvarez, S.A., 1996, Nuevas edades isotópicas de la cubierta volcánica cenozoica de la parte meridional de la Mesa Central, México: Revista Mexicana de Ciencias Geológicas, 13 (1), 117-122.

Ortiz-Hernández, E., Talavera, O., Lapierre, H., Monod, O., Tardy, M., Yta, M., 1991a, Origine intra-océanique des formations volcano-plutoniques d´arc du Jurassique supérieur-Crétacé inférieur du Mexique centro-méridional: Comptes Rendus de l´Académie des Sciences, Serie II, 321, 399-406.

Ortiz-Hernández, E., Lapierre, H., Yta, M., 1991b, Late Jurassic-early Cretaceous tholeiitic and calc-alkaline series in México; implications for the magmatic evolution of the Mexican cordillera (abstract), *en* Convención sobre la Evolución Geológica de México y Primer Congreso Mexicano de Mineralogía. Memoria: Pachuca, Hgo., Universidad Nacional Autónoma de México, Instituto de Geología; Universidad Autónoma del Estado de Hidalgo, Instituto de Investigaciones en Ciencias de la Tierra; Sociedad Mexicana de Mineralogía; Secretaria de Educación Pública, Subsecretaría de Educación Superior e Investigación Científica, 147-149.

Papike, J.J., Cameron, K.L., Baldwin, K., 1974, Amphiboles and pyroxenes: Characterization of other than quadrilateral components and estimates of ferric iron from microprobe data: Geological Society America, Abstracts with Programs, 6, 1053-1054.

Pearce, J.A., 1983, Role of the sub-continental lithosphere in magma genesis at active continental margins, *in* Hawkesworth, C.J., and Norry, M.J. (eds.), Continental basalts and mantle xenoliths: Nantwich, Shiva Publishing, 297-308.

Pérez-Venzor, J.A., Aranda-Gómez, J.J., McDowell, F., Solorio-Munguía, J.G., 1996, Geología del volcán Palo Huérfano, Guanajuato, México: Revista Mexicana de Ciencias Geológicas, 13, 2, 174-183.

Perfit, M.R., Gust, D.A., Bence, A.E., Arculus, R.J., Taylor, S.R., 1980, Chemical characteristics of island-arc basalts; implications for mantle source: Chemical Geology, 30, 227-256.

Robinson, P., Spears, F.S., Schumacher, J.C., Laird, J., Klein, C., Evans, B.W., Doolan, B.L., 1982, Phase relations of metamorphic amphiboles: natural occurrence and theory, *in* Veblen, D. R., Ribbe, P.H. (eds.), Amphiboles; petrology and esperimental phase relations: Washington, D.C., Mineralogical Society of America, Reviews in Mineralogy, 9B, 1-227.

Semet, M.P., Ernst, W.G., 1981, Experimental stability relations of the hornblende magnesiohastingsite: summary: Geological Society of America Bulletin, 92, 71-74.

Talavera-Mendoza, O. Ramírez-Espinosa, J., Guerrero-Suástegui, M., 1995, Petrology and geochemistry of the Teloloapan subterrane: a lower Cretaceous evolved intra-oceanic island arc: Geofísica Internacional, 34 (1), 3-22.

Tardy, M., Maury, R., 1973, Sobre la presencia de elementos de origen volcánico en las areniscas de los flyschs de edad cretácica superior de los estados de Coahuila y Zacatecas: Boletín de la Sociedad Geológica Mexicana, 34 (1-2), 5-12.

Thomas, W.M., 1982, Stability relations of the amphibole hastingsite: American Journal of Science, 282, 136-164.

Manuscript received: January 10, 2001
Corrected manuscript received: January 28, 2002
Manuscript accepted: March 7, 2002